

Diffusion of solitons in anisotropic Heisenberg models

C. Schuster^{1,a}, M. Meister², and F.G. Mertens¹

¹ Physikalisches Institut, Universität Bayreuth, 95440 Bayreuth, Germany

² Departamento de Matemática Aplicada, Universidad Complutense, 28040 Madrid, Spain

Received 19 July 2004

Published online 23 December 2004 – © EDP Sciences, Società Italiana di Fisica, Springer-Verlag 2004

Abstract. We are interested in the thermal diffusion of a solitary wave in the anisotropic Heisenberg spin chain (HSC) with nearest-neighbor exchange interactions. The shape of the solitary wave is approximated by soliton solutions of the continuum HSC with on-site anisotropy, restricting ourselves to large width excitations. Temperature is simulated by white noise coupled to the system. The noise affects the shape and position of the solitary wave and produces magnons. Using implicit collective variables we describe the former effects and neglect magnons (i.e. we use the so-called adiabatic approximation). We derive stochastic equations of motion for the collective variables which we treat both analytically and numerically. Predictions for the mean values and the variances of the variables obtained from these equations are compared with the corresponding results from spin dynamics simulations. For the soliton position we find reasonable agreement between spin dynamics and the results of the collective variable treatment, whereas we observe deviations for the other collective variables. The stochastic dynamics of the position shows both a standard Brownian and a super-diffusive component. These results are analogous to results for the isotropic case, previously studied by some of the authors. In the present article we discuss in particular how the anisotropy enters the stochastic equations of motion and the quantitative changes it causes to the diffusion.

PACS. 05.40.-a Fluctuation phenomena, random processes, noise, and Brownian motion – 75.10.Hk Classical spin models – 05.45.Yv Solitons – 75.30.Gw Magnetic anisotropy

1 Introduction

Coherent nonlinear excitations play an important role in many physical disciplines, see for example [1, 2]. Localized coherent excitations are referred to as solitary waves, whereas the term soliton, in strict usage, is reserved for those solitary waves which are solutions of integrable equations of motion. Integrability is a very strong requirement, thus most physical models are not integrable. If there exists a localized excitation in such a model it is a solitary wave and not a soliton. However, for models that differ from integrable ones by small perturbations only, the soliton of the unperturbed model may serve as a good approximation of the solitary wave of the perturbed system. Coherent excitations are classified as either topological or non-topological. Standard examples of topological excitations are the kink solutions of the sine-Gordon model (integrable) or the Φ^4 model (not integrable). Further examples include the Belavin-Polyakov soliton in the 2d isotropic Heisenberg model and vortices in 2d easy-plane spin systems [3]. Reference [4] contains a discussion on topological and non-topological excitations in the context of magnetic systems.

Thermal fluctuations belong to the most important class of stochastic perturbations. These effects of temperature are often modelled by Gaussian white noise terms, appearing as additional stochastic forces in the otherwise deterministic dynamical equations of a system, see for example [5–7] and references therein.

In this article our goal is to discuss the diffusion of non-topological solitary waves in a HSC with isotropic exchange interaction and on-site (single ion) anisotropy. The analogous problem in the case of only an isotropic exchange interaction was studied in [8, 9] by a collective variable approach similar to the one we use in this paper. In the isotropic case the diffusive motion of the soliton was found to consist of two contributions: a direct effect of the noise on the soliton position (leading to a term in the variance of the position with a linear time dependence) and a part due to noise-induced changes of the soliton velocity (giving a term with cubic time dependence in the variance). Qualitatively we find the same behavior in this work for the anisotropic case. We will demonstrate how the equations of motion are changed by the on-site anisotropy and how the various diffusion coefficients quantitatively depend on the anisotropy.

Furthermore we will show how anisotropy affects the soliton shape in its stability under thermal fluctuations.

^a e-mail: christian.schuster@uni-bayreuth.de

These effects of the anisotropy are connected with difficulties occurring in the spin dynamic simulations which are explained in the fourth section of this paper. The Hamiltonian of the model is

$$\begin{aligned} H &= -J \sum_{n=1}^{N-1} (\mathbf{S}_n \cdot \mathbf{S}_{n+1}) - J \sum_{n=1}^N \frac{\beta}{2} (S_n^z)^2 \\ &= -J \sum_{n=1}^{N-1} (S_n^x S_{n+1}^x + S_n^y S_{n+1}^y + S_n^z S_{n+1}^z) \\ &\quad - J \sum_{n=1}^N \frac{\beta}{2} (S_n^z)^2. \end{aligned} \quad (1)$$

The index n enumerates the spins in the chain with the Cartesian components S_n^x , S_n^y , S_n^z where N is the total number of spins in the chain. The lattice constant is set to unity, the dimensionless quantity J describes the exchange coupling in units of an arbitrarily chosen positive constant J_0 and S measures the spin-length in units of an arbitrarily chosen positive constant S_0 . Thus the energies are measured in units of $J_0 S_0^2$ and the time in units of $\frac{\hbar}{J_0 S_0^2}$. In the continuum approximation the spins $\mathbf{S}_n(t)$ are replaced with $\mathbf{S}(r, t)$ and the Hamiltonian takes the following form:

$$H = \frac{J}{2} \int [\partial_r \mathbf{S} \cdot \partial_r \mathbf{S} - \beta (S^z)^2] dr. \quad (2)$$

The time derivative of \mathbf{S}_n is described by the Landau-Lifshitz equation (LLE)

$$\frac{d}{dt} \mathbf{S}_n = -\mathbf{S}_n \times \mathbf{B}_n, \quad (3)$$

where we define the vector \mathbf{B}_n as $(\mathbf{B}_n)^a := \frac{\partial H}{\partial S_n^a}$ so that $\mathbf{B}_n = -J(\mathbf{S}_{n-1} + \mathbf{S}_{n+1} + \beta S_n^z \hat{e}_z)$. In the continuum version the LLE takes the form

$$\partial_t \mathbf{S}(r, t) = J \mathbf{S}(r, t) \times (\partial_r^2 \mathbf{S}(r, t) + \beta S^z \hat{e}_z). \quad (4)$$

The spin field is described in spherical polar coordinates

$$\begin{aligned} \mathbf{S} &= \{S^x; S^y; S^z\} \\ &= \left\{ \sqrt{S^2 - (S^z)^2} \cos \Phi; \sqrt{S^2 - (S^z)^2} \sin \Phi; S^z \right\}, \end{aligned} \quad (5)$$

where $S^z = S \cos(\Theta)$, and Θ is the polar and Φ the azimuthal angle. The isotropic case ($\beta = 0$) was investigated in [8, 9]. The soliton solution of (4) for this case is

$$\cos(\Theta(r, t)) = 1 - A \left[\operatorname{sech} \left(\frac{r - X(t)}{\Gamma} \right) \right]^2, \quad (6)$$

$$\begin{aligned} \Phi(r, t) &= \Phi_0 + \omega t \pm \sqrt{\frac{2}{A} - 1} \frac{r - X(t)}{\Gamma} \\ &\quad + \arctan \left[\pm \sqrt{\frac{A}{2-A}} \tanh \left(\frac{r - X(t)}{\Gamma} \right) \right]. \end{aligned} \quad (7)$$

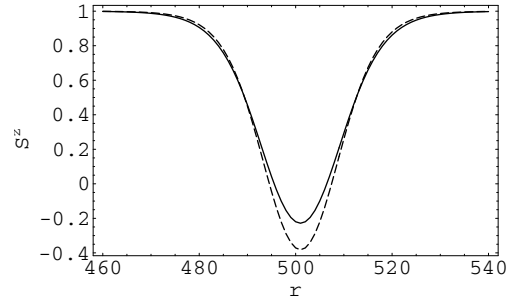


Fig. 1. S^z in dependence on r with parameters $A = 1, \Gamma = 20$ (dashed line), and $A = 0.38, \Gamma = 38.72$ (solid line), with anisotropy $\beta = 0.01$.

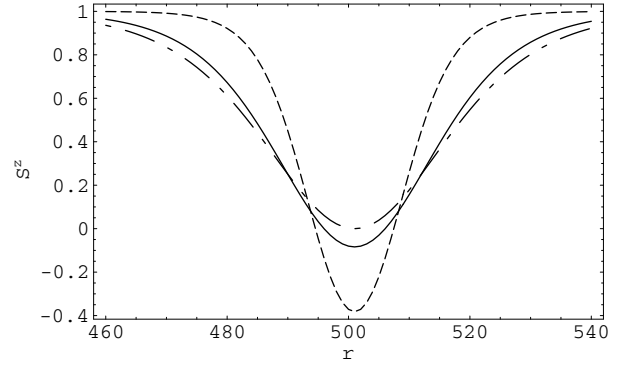


Fig. 2. S^z -component, $\beta = 0.01$ (dashed line), $\beta = 0.001$ (solid line) and $\beta = 0.00$ (dash-dotted line), $\Gamma = 20, A = 1$.

The parameters A and Γ denote the amplitude and the width of this soliton. $X(t) = X_0 + Vt$ describes the position of the soliton at time t , where $V = \frac{2JS}{\Gamma} \sqrt{\frac{2-A}{A}}$ describes the constant speed (when the system is unperturbed). For $\beta \neq 0$ the soliton solution of (4) is mentioned in [4]. As a short notation we define $\xi = r - X(t)$ and get

$$\begin{aligned} \frac{S^z}{S} &= \cos \Theta(\xi) = \\ &= 1 - \frac{2A(1 + \beta\Gamma^2)}{1 + A\beta\Gamma^2 + \sqrt{1 + (2-A)A\beta\Gamma^2} \cosh(2\sqrt{\beta+1/\Gamma^2}\xi)} \end{aligned} \quad (8)$$

$$\begin{aligned} \Phi(\xi) &= \Phi_0(t) + \sqrt{\frac{1}{\Gamma^2} \frac{2-A}{A}} \xi \\ &\quad + \arctan \left[\frac{\sqrt{\beta\Gamma^2 + 1} \sqrt{(2-A)A} \tanh(\sqrt{\beta + \Gamma^{-2}}\xi)}{1 - A + \sqrt{1 + (2-A)A\beta\Gamma^2}} \right]. \end{aligned} \quad (9)$$

In the limit $\beta \rightarrow 0$ we recover (6) and (7), see Figure 2.

One may easily observe in Figures 1 and 2 that the system parameter β has a much larger effect on the structure of the soliton than the soliton parameters A and Γ . As a consequence of the relatively large anisotropy ($\beta = 0.01$) even large changes in A and Γ only result in small structural changes of S^z , and vice versa even small changes

in the structure correspond to huge changes in A and Γ . Larger β values result in a narrower soliton pulse, and vice versa smaller β values result in a broader soliton pulse which approaches the soliton pulse obtained from the isotropic HSC.

The diffusive motion of the solitary wave is due to a coupling of the system to a thermal bath which we model by including Gilbert damping and white noise terms into the equations of motion in the following way:

$$\frac{d}{dt}\mathbf{S}_n + \varepsilon\mathbf{S}_n \times \frac{d}{dt}\mathbf{S}_n = -\mathbf{S}_n \times \mathbf{B}_n - \mathbf{S}_n \times \mathbf{b}_n \quad (10)$$

and in the continuum version

$$\frac{\partial}{\partial t}\mathbf{S} + \varepsilon\mathbf{S} \times \frac{\partial}{\partial t}\mathbf{S} = -\mathbf{S} \times \mathbf{B} - \mathbf{S} \times \mathbf{b}. \quad (11)$$

The second term on the LHS represents the Gilbert damping. The vector \mathbf{b} on the RHS of the equation describes Gaussian white noise, satisfying

$$\begin{aligned} \langle \mathbf{b}_n(t) \rangle &= 0, \\ \langle b_m^i(t_1)b_n^j(t_2) \rangle &= \sigma^2\delta_{mn}\delta^{ij}\delta(t_1 - t_2) \end{aligned} \quad (12)$$

and in the continuum case

$$\begin{aligned} \langle \mathbf{b}(r, t) \rangle &= 0, \\ \langle b^i(r_1, t_1)b^j(r_2, t_2) \rangle &= \sigma^2\delta^{ij}\delta(r_1 - r_2)\delta(t_1 - t_2). \end{aligned} \quad (13)$$

While damping dissipates energy, the noise transfers energy to the chain from a thermal bath. For temperatures $k_B T/JS^2 \ll 1$ the average thermal energy per pair of neighboring spins is $k_B T$ and according to the fluctuation-dissipation relation $\sigma^2 = 2\varepsilon k_B T$; for a detailed discussion see [8].

We discuss the effects of the perturbative terms in adiabatic approximation, i.e. we neglect magnons generated by the thermal fluctuations and consider only the effects on the solitary wave as a whole. That can be conveniently done with collective variables [10–12]. We use implicit collective variables that arise by allowing for a perturbation-induced time dependence of time-independent parameters of the unperturbed solution. In Section 2 we consider the short-time behavior, which allows us to neglect damping. We derive stochastic equations of motion (SEM) for the collective variables and solve them perturbatively. In Section 3 damping is included and the discussion is extended to a longer time period. A different set of SEM for the collective variables is derived in this section which will be solved numerically later. Section 4 explains our method of determining the collective variables from spin dynamics simulations. In Section 5 we compare these results with the numerical solution of the SEM from Section 3 and the results from Section 2. Section 6 summarizes our results.

2 Short time periods

In this section we neglect damping. The results will only apply to a short time period as we do not take into account

the time dependent changes of the collective variables due to damping.

We make the following ansatz with time dependent quantities X, A, Γ and Φ_0 (implicit collective variables).

$$\mathbf{S}(r, t) = \mathbf{S}_{sol}(r - X(t), \Phi_0(t), A(t), \Gamma(t)), \quad (14)$$

where \mathbf{S}_{sol} refers to the analytical solutions (8) and (9). Inserting this ansatz into (11) with $\varepsilon = 0$ and considering only the z -component of this equation we get

$$\begin{aligned} \frac{\partial S_{sol}^z}{\partial X} \dot{X} + \frac{\partial S_{sol}^z}{\partial A} \dot{A} + \frac{\partial S_{sol}^z}{\partial \Gamma} \dot{\Gamma} &= J [\mathbf{S}_{sol} \times \partial_r^2 \mathbf{S}_{sol}]^z, \\ &- [\mathbf{S}_{sol} \times \mathbf{b}]^z. \end{aligned} \quad (15)$$

As S^z is independent of Φ_0 we only consider the dynamics of X, A and Γ . As an abbreviation we write $\frac{S^z}{S} = f$. We multiply (15) by $\partial f/\partial X, \partial f/\partial A$ and $\partial f/\partial \Gamma$, respectively, and integrate over r . Thus we arrive at a system of ordinary stochastic differential equations:

$$\begin{aligned} \begin{bmatrix} b_{11} & 0 & 0 \\ 0 & b_{22} & b_{23} \\ 0 & b_{23} & b_{33} \end{bmatrix} \begin{bmatrix} \dot{X} \\ \dot{A} \\ \dot{\Gamma} \end{bmatrix} &= \begin{bmatrix} \int \frac{\partial \Psi}{\partial r} \frac{\partial}{\partial r} [(1-f^2) \frac{d\Phi}{dr}] dr \\ 0 \\ 0 \end{bmatrix} \\ &- \begin{bmatrix} \int \frac{\partial f(r, A, \Gamma)}{\partial X} [\mathbf{S}_{sol} \times \mathbf{b}]^z dr \\ \int \frac{\partial f(r, A, \Gamma)}{\partial A} [\mathbf{S}_{sol} \times \mathbf{b}]^z dr \\ \int \frac{\partial f(r, A, \Gamma)}{\partial \Gamma} [\mathbf{S}_{sol} \times \mathbf{b}]^z dr \end{bmatrix}, \end{aligned} \quad (16)$$

with

$$b_{ij} = \int \frac{\partial f}{\partial U_i} \frac{\partial f}{\partial U_j} dr \quad (17)$$

and $U_i, i \in \{1, 2, 3\}$ denoting the collective variables X, A and Γ . After inversion of the system (16) we obtain:

$$\begin{aligned} \dot{X} &= \frac{2JS}{\Gamma} \sqrt{\frac{2}{A} - 1} + F_X^{st}, \\ \dot{A} &= F_A^{st}, \\ \dot{\Gamma} &= F_\Gamma^{st}, \end{aligned} \quad (18)$$

where F^{st} denote stochastic forces reflecting the effects of noise coupled to the spins. We note that for vanishing stochastic forces we recover the correct behavior of X, A and Γ of the unperturbed case. As we restrict our system to small noise we thus may treat collective variables and noise terms as approximately stochastically independent from each other (a detailed discussion can be found in [8]), which leads to $\langle F_U^{st} \rangle = 0$ with $U = X, A, \Gamma$. The correlations of the stochastic forces are:

$$\begin{aligned} \langle F_X^{st}(t_1)F_A^{st}(t_2) \rangle &= 0, \\ \langle F_X^{st}(t_1)F_\Gamma^{st}(t_2) \rangle &= 0 \end{aligned} \quad (19)$$

and some expressions which we could not evaluate explicitly, such as

$$\begin{aligned} \langle F_A^{st}(t_1) F_A^{st}(t_2) \rangle &= \frac{\sigma^2 \delta(t_1 - t_2)}{(b_{23}^2 - b_{22} b_{23})^2} \\ &\times \int_{-\infty}^{+\infty} \left(b_{33} \frac{\partial}{\partial A} f(r, A, \Gamma) - b_{23} \frac{\partial}{\partial \Gamma} f(r, A, \Gamma) \right)^2 \\ &\quad (1 - f^2(r, A, \Gamma)) dr. \end{aligned}$$

They are evaluated numerically when necessary. As an abbreviation we define

$$\langle F_U^{st}(t_1) F_V^{st}(t_2) \rangle = \sigma^2 \delta(t_1 - t_2) \langle \Sigma_{UV}(A, \Gamma) \rangle. \quad (20)$$

The structure of the collective variable equations does not differ from the isotropic case. The only difference due to the anisotropy occurs in the diffusion coefficients $\langle \Sigma_{UV}(A, \Gamma) \rangle$. Therefore we proceed as in [8, 9]. Using mutually independent Wiener processes W_X , W_1 and W_2 we express the stochastic equations of motion without damping (SEM 1) as follows:

$$\begin{aligned} dX &= \frac{2JS}{\Gamma} \sqrt{\frac{2}{A}} - 1 dt + \sigma \alpha(A, \Gamma) dW_X, \\ dA &= \sigma \beta_1(A, \Gamma) dW_1, \\ d\Gamma &= \sigma \gamma_1(A, \Gamma) dW_1 + \sigma \gamma_2(A, \Gamma) dW_2, \end{aligned} \quad (21)$$

where

$$\begin{aligned} \alpha &= \sqrt{\Sigma_{XX}}, \quad \beta_1 = \sqrt{\Sigma_{AA}}, \\ \gamma_1 &= \frac{\Sigma_{A\Gamma}}{\sqrt{\Sigma_{AA}}}, \quad \gamma_2 = \sqrt{\Sigma_{\Gamma\Gamma} - \frac{\Sigma_{A\Gamma}^2}{\Sigma_{AA}}}. \end{aligned} \quad (22)$$

The system of equations (21) is solved analytically by using the perturbative technique of small noise expansion [13] for X , A and Γ . Details are explained in [8, 9]. The solutions to the first order of σ are:

$$\begin{aligned} \text{Var}[X(t)] &= \sigma^2 \Sigma_{XX} t + \sigma^2 \Sigma_{cub} t^3, \\ \text{Var}[A(t)] &= \sigma^2 \Sigma_{AA} t, \\ \text{Var}[\Gamma(t)] &= \sigma^2 \Sigma_{\Gamma\Gamma} t, \end{aligned} \quad (23)$$

where

$$\begin{aligned} \Sigma_{cub} &= \frac{4J^2 S^2}{3\Gamma_0^2} \\ &\times \left[\frac{\Sigma_{AA}}{A_0^4} \left(\frac{2}{A_0} - 1 \right)^{-1} + \frac{\Sigma_{\Gamma\Gamma}}{\Gamma_0^2} \left(\frac{2}{A_0} - 1 \right) + \frac{2\Sigma_{A\Gamma}}{A_0^2 \Gamma_0} \right]. \end{aligned} \quad (24)$$

The coefficients Σ_{UV} depend only on A and Γ and are evaluated here (numerically) for the initial values of these variables; that results from the perturbative calculation. We observe a *direct effect* from the noise on the position: a usual *random walk* leads to a linear time behavior of $\text{Var}(X)$. In addition, we observe an *indirect effect*:

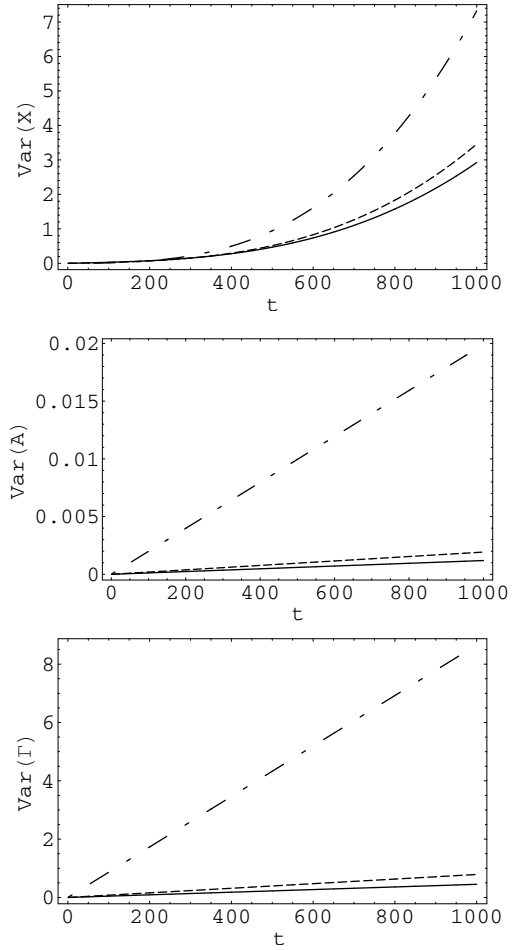


Fig. 3. Variances in equation (23): $\text{Var}(X)$, $\text{Var}(A)$ and $\text{Var}(\Gamma)$ depending on t , $k_B T = 0.001$ with anisotropy $\beta = 0.01$ (dash-dotted), $\beta = 0.001$ (dashed) and $\beta = 0.0001$ (solid line), in all figures the initial values are $A = 1$, $\Gamma = 20$.

The noise changes A and Γ . In fact, we obtain for these variables a linear time dependence in the variances which corresponds to an ordinary *random walk*. As A and Γ determine the velocity of the excitation, their stochastic dynamics result in stochastic velocity changes. This phenomenon leads to an additional term in the variance of the position that grows as t^3 . The same behavior of the variances of the collective variables on time was encountered in the isotropic case [8, 9]. However, the values of the diffusion coefficients multiplying the powers of t depend on β as we now discuss.

As we already mentioned in Section 1 small fluctuations in the structure lead to large fluctuations in A and Γ , which increase with β . This relationship leads to larger fluctuations in the velocity V and conterminously an increase of Σ_{cub} . In Figure 3 we observe this effect β has, an increase of anisotropy leads to an increase in the variances. That means that at a given temperature fluctuations in the structure lead to larger fluctuations in A and Γ with higher β values. This relationship is verified by the plots of the diffusion constants Σ_{XX} , Σ_{cub} , Σ_{AA} and $\Sigma_{\Gamma\Gamma}$ in dependence of β . From Figure 4 one may

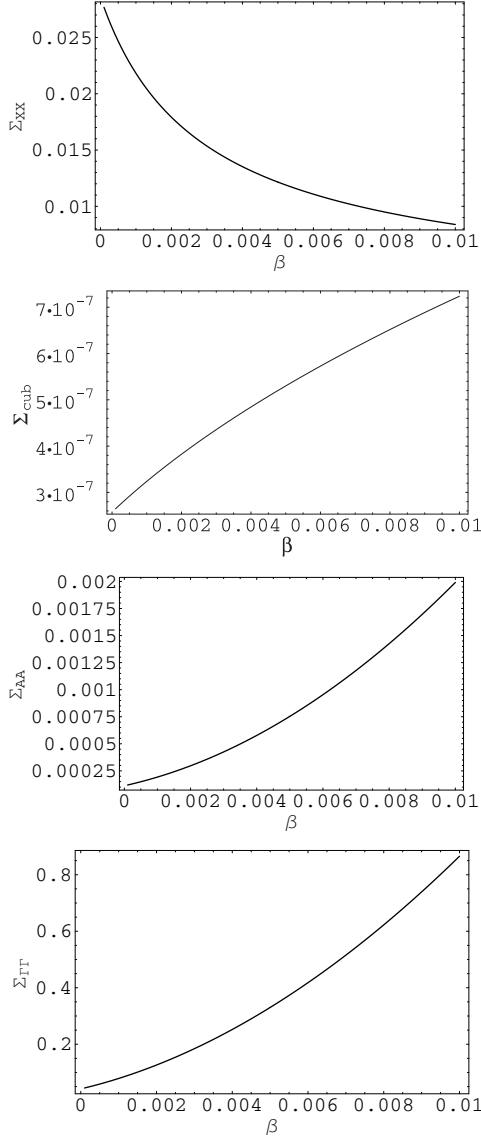


Fig. 4. Diffusion constants in equations (23): Σ_{XX} , Σ_{cub} (coefficient of the cubic part in $Var(X)$), Σ_{AA} and $\Sigma_{\Gamma\Gamma}$ depending on β for constant $A = 1$, $\Gamma = 20$, $\Sigma_{A\Gamma}$ is not displayed as it is already contained in Σ_{cub} , which has a direct effect on $Var(X)$.

observe that all diffusion constants of equation (23) increase with increasing β , except for Σ_{XX} . This exception is quickly compensated for by the cubic component Σ_{cub} so that for $t > 100$ $Var(X)$ increases with an increasing β value. Furthermore this behavior of increasing variances with increasing anisotropy is valid for all possible sets of parameter values for A and Γ .

3 Long time periods

In this section we include the Gilbert damping term ($\varepsilon \neq 0$) in the Landau-Lifshitz-equation (11) in addition to the noise. Hence the equations of motion derived here

are applicable for a longer time period than the results in Section 2. In the LLE with noise and Gilbert-damping

$$\frac{\partial}{\partial t} \mathbf{S} + \varepsilon \mathbf{S} \times \frac{\partial}{\partial t} \mathbf{S} = -\mathbf{S} \times \mathbf{B} - \mathbf{S} \times \mathbf{b}$$

we again insert the ansatz (14)

$$\mathbf{S}(r, t) = \mathbf{S}_{sol}(r - X(t), \Phi_0(t), A(t), \Gamma(t)).$$

This results in

$$\sum_{i=1}^4 \left(\frac{\partial \mathbf{S}_{sol}}{\partial U_i} + \varepsilon \mathbf{S}_{sol} \times \frac{\partial \mathbf{S}_{sol}}{\partial U_i} \right) \dot{U}_i = -\mathbf{S}_{sol} \times (\mathbf{B} + \mathbf{b}) \quad (25)$$

where $i, k \in \{1, 2, 3, 4\}$ and $U_1 := X$, $U_2 := \Phi_0$, $U_3 := A$ and $U_4 := \Gamma$. We take a vector product for the above equation with $\frac{\partial \mathbf{S}_{sol}}{\partial U_k}$ and afterwards the scalar product of the result with \mathbf{S}_{sol} and integrate over all space:

$$\begin{aligned} \sum_{i=1}^4 \int \mathbf{S}_{sol} \cdot \left[\frac{\partial \mathbf{S}_{sol}}{\partial U_k} \frac{\partial \mathbf{S}_{sol}}{\partial U_i} + \varepsilon \frac{\partial \mathbf{S}_{sol}}{\partial U_k} \right. \\ \left. \times \left(\mathbf{S}_{sol} \times \frac{\partial \mathbf{S}_{sol}}{\partial U_i} \right) \right] dr \dot{U}_i \\ = - \int \mathbf{S}_{sol} \cdot \left[\frac{\partial \mathbf{S}_{sol}}{\partial U_k} \times (\mathbf{S}_{sol} \times (\mathbf{B} + \mathbf{b})) \right] dr. \quad (26) \end{aligned}$$

We introduce the vector $\mathbf{C} := \mathbf{C}^{in} + \mathbf{C}^{ex}$ defined by:

$$\begin{aligned} C_k^{in} &:= - \int \mathbf{S}_{sol} \cdot \left[\frac{\partial \mathbf{S}_{sol}}{\partial U_k} \times (\mathbf{S}_{sol} \times \mathbf{B}) \right] dr, \\ C_k^{ex} &:= - \int \mathbf{S}_{sol} \cdot \left[\frac{\partial \mathbf{S}_{sol}}{\partial U_k} \times (\mathbf{S}_{sol} \times \mathbf{b}) \right] dr. \quad (27) \end{aligned}$$

Using rules of vector algebra the transformed LLE (25) may be written as:

$$\sum_{i=1}^4 [N_{ki} + \varepsilon M_{ki}] \dot{U}_i = \sum_{i=1}^4 L(\varepsilon) \dot{U}_i = C_k, \quad (28)$$

where

$$\begin{aligned} N_{ki} &:= \int \mathbf{S}_{sol} \cdot \left[\frac{\partial \mathbf{S}_{sol}}{\partial U_k} \times \frac{\partial \mathbf{S}_{sol}}{\partial U_i} \right] dr, \\ M_{ki} &:= S^2 \int \frac{\partial \mathbf{S}_{sol}}{\partial U_k} \cdot \frac{\partial \mathbf{S}_{sol}}{\partial U_i} dr. \quad (29) \end{aligned}$$

After inverting the system we get

$$\dot{U}_i = \sum_{k=1}^4 [\mathbf{L}(\varepsilon)^{-1}]_{ik} C_k. \quad (30)$$

Writing (30) explicitly we get

$$\begin{bmatrix} \dot{X} \\ \dot{\Phi}_0 \\ \dot{A} \\ \dot{\Gamma} \end{bmatrix} = \begin{bmatrix} \varepsilon M_{11} & \varepsilon M_{12} & N_{13} & N_{14} \\ \varepsilon M_{12} & \varepsilon M_{22} & N_{23} & N_{24} \\ -N_{13} & -N_{23} & \varepsilon M_{33} & \varepsilon M_{34} \\ -N_{14} & -N_{24} & \varepsilon M_{34} & \varepsilon M_{44} \end{bmatrix}^{-1} \begin{bmatrix} 0 + C_X^{ex} \\ 0 + C_{\Phi_0}^{ex} \\ C_A^{in} + C_A^{ex} \\ C_\Gamma^{in} + C_\Gamma^{ex} \end{bmatrix} \quad (31)$$

where

$$N_{ki} = S^3 \int \left[\frac{\partial \Psi_c}{\partial U_i} \frac{\partial \Phi_c}{\partial U_k} - \frac{\Psi_c}{\partial U_k} \frac{\partial \Phi_c}{\partial U_i} \right] dr,$$

$$M_{ki} = S^4 \int \left[\frac{1}{1 - \Psi_c^2} \frac{\partial \Psi_c}{\partial U_k} \frac{\partial \Psi_c}{\partial U_i} + (1 - \Psi_c^2) \frac{\partial \Phi_c}{U_k} \frac{\partial \Phi_c}{\partial U_i} \right] dr \quad (32)$$

and

$$C_k^{in} = JS^4 \int \left[\frac{\partial \Phi}{\partial U_k} \frac{d}{d\xi} [2k(1-f)] + \frac{1}{2} \left[\left(\frac{d\Phi}{d\xi} \right)^2 + \frac{\beta}{\alpha} \right] \frac{\partial}{\partial U_k} f^2 + \frac{d^2 \Theta}{d\xi^2} \frac{\partial \Theta}{\partial U_k} \right] dr,$$

$$C_k^{ex} = -S^2 \int \mathbf{b} \cdot \frac{\partial \mathbf{S}_{sol}}{\partial U_k} dr. \quad (33)$$

Explicitly we obtain $C_X^{in} = 0$, $C_{\Phi_0}^{in} = 0$, $M_{ij} = M_{ji}$, $N_{ij} = -N_{ji}$ and

$$M_{11} = \frac{4S^4}{A\Gamma^2 \sqrt{\beta}} \left(A\Gamma \sqrt{\beta(1+\beta\Gamma^2)} - \log \left[\frac{1 + A\beta\Gamma^2 - A\Gamma \sqrt{\beta(1+\beta\Gamma^2)}}{\sqrt{1 - (-2+A)A\beta\Gamma^2}} \right] \right),$$

$$M_{12} = \frac{4S^4}{\sqrt{\beta}\Gamma} \sqrt{\frac{2-A}{A}} \log \left[\frac{1 + A\beta\Gamma^2 - A\Gamma \sqrt{\beta(1+\beta\Gamma^2)}}{\sqrt{1 - (-2+A)A\beta\Gamma^2}} \right],$$

$$M_{22} = \frac{4S^4}{\beta\sqrt{\beta}A\Gamma^2} \left(A\Gamma \sqrt{\beta(1+\beta\Gamma^2)} + \log \left[\frac{1 + A\beta\Gamma^2 - A\Gamma \sqrt{\beta(1+\beta\Gamma^2)}}{\sqrt{1 - (-2+A)A\beta\Gamma^2}} \right] \right),$$

$$N_{23} = \frac{S^3 2(1+\beta\Gamma^2)}{\sqrt{\beta+1/\Gamma^2}(-1 - (-2+A)A\beta\Gamma^2)},$$

$$N_{24} = \frac{S^3 2A(-1 + (-2+A)\beta\Gamma^2)}{\sqrt{\beta\Gamma^2+1}(1 - (-2+A)A\beta\Gamma^2)}.$$

M_{33} , M_{34} , M_{44} , N_{13} and N_{14} are calculated numerically as well as D_{ij} which are all defined below. We define the intrinsic and stochastic forces

$$F_i^{in} := \sum_{k=1}^4 [\mathbf{L}(\varepsilon)^{-1}]_{ik} C_k^{in},$$

$$F_i^{st} := \sum_{k=1}^4 [\mathbf{L}(\varepsilon)^{-1}]_{ik} C_k^{ex}. \quad (34)$$

The correlations of the stochastic forces are

$$\langle F_i^{ex}(t_1) F_j^{ex}(t_2) \rangle = \sum_{m=1}^4 \sum_{k=1}^4 \left\langle [\mathbf{L}(\varepsilon)^{-1}]_{ik}(t_1) C_k^{ex}(t_1) [\mathbf{L}(\varepsilon)^{-1}]_{jm}(t_2) C_m^{ex}(t_2) \right\rangle. \quad (35)$$

As in Section 2 we neglect possible correlations between the noise and the collective variables. This neglect amounts to dropping a term $\propto \sigma^2$ in the equations of motion and thus is justified for weak noise. We find

$$\langle F_i^{st}(t_1) F_j^{st}(t_2) \rangle = \sigma^2 S^4 \sum_{k=1}^N \sum_{m=1}^N \left\langle [\mathbf{L}(\varepsilon)^{-1}]_{ik}(t_1) [\mathbf{L}(\varepsilon)^{-1}]_{jm}(t_1) \times \int \frac{\partial \mathbf{S}_{sol}}{\partial U_k} \cdot \frac{\partial \mathbf{S}_{sol}}{\partial U_m}(t_1, r) dr \right\rangle \delta(t_1 - t_2)$$

$$= \sigma^2 S^2 \left\langle [\mathbf{L}(\varepsilon)^{-1} \mathbf{M}_G (\mathbf{L}(\varepsilon)^{-1})^T]_{ij}(t_1) \right\rangle \delta(t_1 - t_2)$$

$$=: \langle D_{ij}(t_1) \rangle \delta(t_1 - t_2). \quad (36)$$

The correlation matrix has the following structure:

$$D = \begin{bmatrix} D_{XX} & D_{X\Phi_0} & 0 & 0 \\ D_{X\Phi_0} & D_{\Phi_0\Phi_0} & 0 & 0 \\ 0 & 0 & D_{AA} & D_{A\Gamma} \\ 0 & 0 & D_{A\Gamma} & D_{\Gamma\Gamma} \end{bmatrix}. \quad (37)$$

Also, in this approximation we have $\langle F_i^{st} \rangle = 0$, as can be seen from the definition of F_i^{st} .

Just as in the isotropic case [8, 9] and analogously to Section 2 we introduce mutually independent Wiener processes and find the stochastic equations of motion with damping (SEM 2)

$$dX = F_X^{in} dt + \alpha_1 dW_1 + \alpha_2 dW_2,$$

$$d\Phi_0 = F_{\Phi_0}^{in} dt + \alpha_3 dW_2,$$

$$dA = F_A^{in} dt + \alpha_4 dW_3 + \alpha_5 dW_4,$$

$$d\Gamma = F_\Gamma^{in} dt + \alpha_6 dW_4, \quad (38)$$

where

$$\alpha_1 = \sqrt{D_{11} - \frac{D_{12}^2}{D_{22}}}, \quad \alpha_2 = \frac{D_{12}}{\sqrt{D_{22}}}, \quad \alpha_3 = \sqrt{D_{22}},$$

$$\alpha_4 = \sqrt{D_{33} - \frac{D_{34}^2}{D_{44}}}, \quad \alpha_5 = \frac{D_{34}}{\sqrt{D_{44}}}, \quad \alpha_6 = \sqrt{D_{44}}. \quad (39)$$

Expanding these coefficients into a Taylor-series it is easily seen that in the approximation

$$\langle \alpha_i(\dots, U_k, \dots) \rangle \approx \alpha_i(\dots, \langle U_k \rangle, \dots) \quad (40)$$

the error is of the order of σ^2 .

As our system of equations (38) is correct to an order of σ^1 only they can be simplified from

$$dU_i = F_i^{in}(\dots, U_k, \dots) dt + \sum_s \alpha_s^{(i)}(\dots, U_k, \dots) dW_s, \quad (41)$$

to

$$dU_i = F_i^{in}(\dots, U_k, \dots)dt + \sum_s \alpha_s^{(i)}(\dots, \langle U_k \rangle, \dots)dW_s, \quad (42)$$

The dynamics of the expectation values in the same approximation is given by

$$d\langle U_i \rangle = F_i^{in}(\dots, \langle U_k \rangle, \dots)dt. \quad (43)$$

Therefore we see that to the order of σ^1 the quantities F_i^{st} are additive white noise with a time dependent strength. This time dependency is determined by the time dependence of the expectation values according to (43). The latter equation corresponds to the equation of motion for the collective variables in the case when only damping and no noise is coupled to the system. The simplified set of equations (42) will be solved numerically and the results will be compared with the simulations.

4 Determination of collective variables in simulations

We solved SEM 1 equation (21) analytically and SEM 2 equation (38) numerically. For comparison the spin dynamics of a chain of 1000 spins was simulated, which is described by the Landau-Lifshitz equation (10). This equation is solved numerically by the Heun algorithm [14]. The solution takes the form of a discrete set of values for S^z in each time step of the simulation. Now we construct an algorithm to detect all collective variables from this set, starting with the position X of the soliton. We define the function

$$F(Y; A_i, \Gamma_i) := \int S^z(r - X, A, \Gamma) \frac{\partial S_c^z}{\partial r}(r - Y, A_i, \Gamma_i) dr. \quad (44)$$

If S^z is a soliton configuration it follows that F must vanish for $Y = X$, regardless of A_i and Γ_i , due to symmetry. We evaluate in the simulations (a discrete version of) the integral in the definition of F where S^z is the simulated spin configuration and S_c^z the soliton solution. As trial values A_i and Γ_i in the first step we use the initial values A_0 and Γ_0 , respectively. We calculate F for a number of trial values Y_i (spaced at 0.25 in a symmetric interval around the previously determined value of X), looking for a change of sign between two subsequent trial values. From this calculation we find the value Y for which F vanishes by linear interpolation, thus obtaining the value of X .

Next we determine the minimal value S_{min}^z of S^z to obtain a relation between A and Γ . For this aim we need a suitable fit. The better the fit function approaches the discrete soliton structure the more accurately we can determine S_{min}^z . As the analytic expression for S^z (8) is too complex for use in a least square fit we thus take a simple pulse $\text{sech}^2(x)$ as the fit function. The minimum of this function is taken as the value of S_{min}^z . Consistent with the adiabatic approximation we also consider the minimum as the value of the soliton solution at X . From this value and

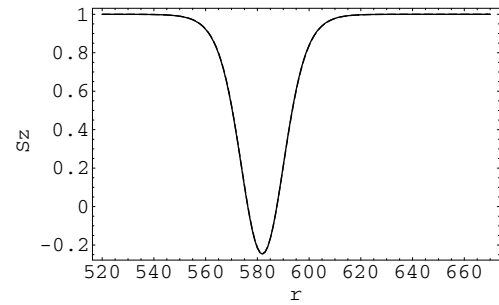


Fig. 5. S^z after 800 time units, dashed line: shape of S^z described by the analytical solution (8), which we fit to the simulated configuration with suitable parameters A and Γ , solid line: S^z from the simulation with initial parameters $A = 1$, $\Gamma = 20$, $\beta = 0.01$, $k_B T = 0$, $\varepsilon = 0.01$, no deviation between these two lines can be seen.

the soliton solution (8) we express A as a function of Γ . Then we define:

$$\Delta(\Gamma_i) = \int [S^z - S_c^z(r - X, A_i(\Gamma_i), \Gamma_i)]^2 dr. \quad (45)$$

Using trial values of Γ_i we search for the value Γ_j which minimizes $\Delta(A_i(\Gamma_i), \Gamma_i)$. Taking this value and $\Gamma_{j\pm 1}$ we fit a parabola to these three points in the Δ - Γ plane. Finding the minimum of this parabola we obtain the demanded value of Γ , along with its corresponding value of A .

With this pair (A, Γ) we determine the definitive value of X in the same way as before. The values of A and Γ just found are used as new initialization values for the next calculation of X in the next time step. Φ_0 can now be easily calculated from (A, Γ) and the actual spin configuration [9].

As we discussed in Section 1, Γ and A are rather sensitive to changes in the structure of the soliton. This fact poses a problem for the determination of these two variables from the simulated spin configuration. The consequences of which will be seen and discussed in the next section.

We have also checked how well the spin configuration is approximated by the ansatz. We take the values of X , A and Γ determined from the simulations (at $k_B T = 0$, $\beta = 0.01$), plug them into the exact soliton solution and compare with the configuration from the simulations. As we can see from Figure 5 there exist no visible differences between these two configurations. The approximation of the ansatz is satisfying and our algorithm for determining the collective variables works well.

5 Numerical results

The stochastic equations of motion with damping SEM 2 (38) for the collective variables are solved numerically with the Heun algorithm [14], which was designed especially for multiplicative noise. We use a time step of 0.1. We insured that the usage of this time step does not visibly affect the accuracy of the results compared to a smaller time step of 0.01. We compare these results with

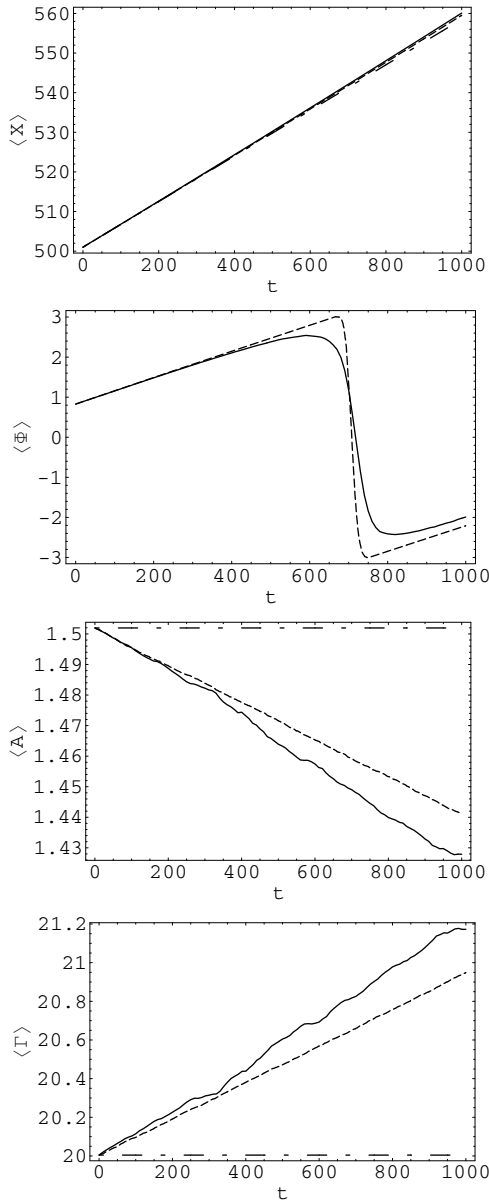


Fig. 6. Mean values of the collective variables, solid line: simulations, dashed line: numerical integration of SEM 2 (38), dash-dotted line: analytical solution of SEM 1 (21), $\beta = 0.001$, $k_B T = 0.001$, $\varepsilon = 0.01$. Initial values used were $A = 1.5$, $\Gamma = 20$, $\Phi_0 = 0.83$.

spin dynamics simulations. The spin dynamics is described by equation (10) which is also solved using the Heun algorithm with a time step of 0.01. This algorithm provides an adequate treatment of multiplicative couplings between the components of the spins and the noise, arising out of $\mathbf{S}_n \times \mathbf{b}_n$.

The collective variables X , Φ_0 , A and Γ are determined by the algorithm described in section 4. In the numerical solution of SEM 2 as well as in the simulations we consider 1000 realizations in the time $t = 1000$ at a temperature of $k_B T = 0.001$ with anisotropy $\beta = 0.001$. Furthermore two different sets of initial soliton parameters Φ_0 , A and Γ are used in the results shown in Figures 6, 7, 8

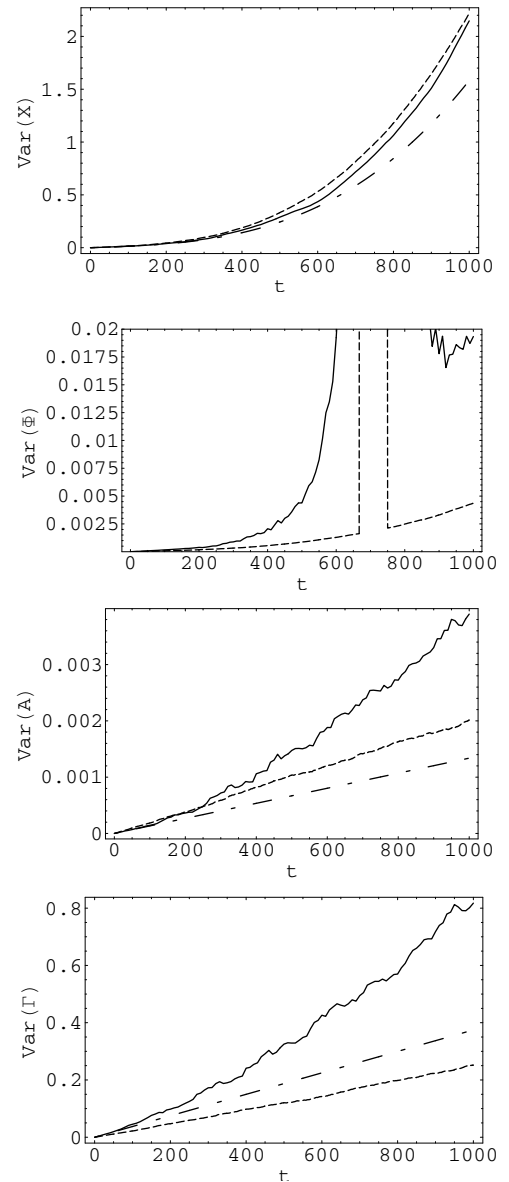


Fig. 7. Variances of the collective variables, solid line: simulations, dashed line: numerical integration of SEM 2 (38), dash-dotted line: analytical solution of SEM 1 (21), $\beta = 0.001$, $k_B T = 0.001$, $\varepsilon = 0.01$. Initial values used were $A = 1.5$, $\Gamma = 20$, $\Phi_0 = 0.83$.

and 9. To describe soliton dynamics the most important variable doubtlessly is the position $X(t)$. In $\langle X \rangle$ as well as in $Var(X)$ we obtain a very good agreement between spin dynamics, the numerical solution of collective variables equations and the perturbative results of Section 2. The mean value of Φ is also well reproduced.

As anticipated, the numerical solution of SEM 2 fits much better to the dynamics than SEM 1 where we neglect the damping after intermediate times ($t \leq 200$). The neglect of the damping in SEM 1 is in fact an unsuitable approximation for a long time period (especially for A and Γ).

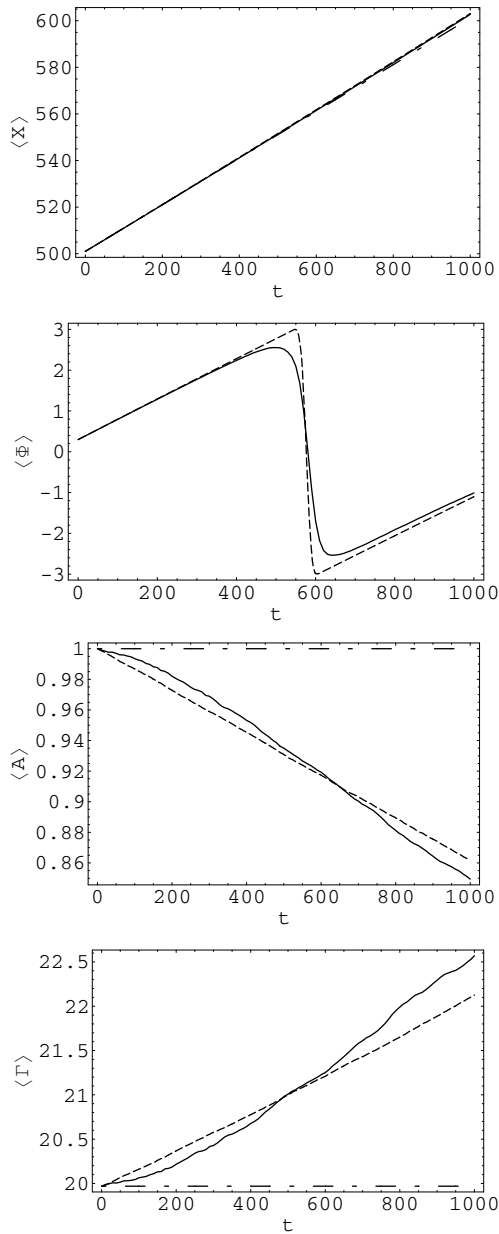


Fig. 8. Mean values of the collective variables, solid line: simulations, dashed line: numerical integration of SEM 2 (38), dash-dotted line: analytical solution of SEM 1 (21), $\beta = 0.001$, $k_B T = 0.001$, $\varepsilon = 0.01$. Initial values used were $A = 1$, $\Gamma = 20$, $\Phi_0 = 0.298$.

The systematic deviations between spin dynamics and SEM2 observed for A and Γ shown in Figures 6, 7, 8 and 9 are a product of the measuring procedure. Spike-like distortions appearing on the sides of the solitary wave increase the width determined by the $\text{sech}^2(x)$ -fit and therefore lead to fluctuations in the minimum S_{min}^z which is directly related to the determination of A and Γ . As already mentioned in the first section as an effect of anisotropy small fluctuations in the soliton shape lead to large fluctuations in A and Γ which makes the measurement of these collective variables even more difficult. These fluctuations

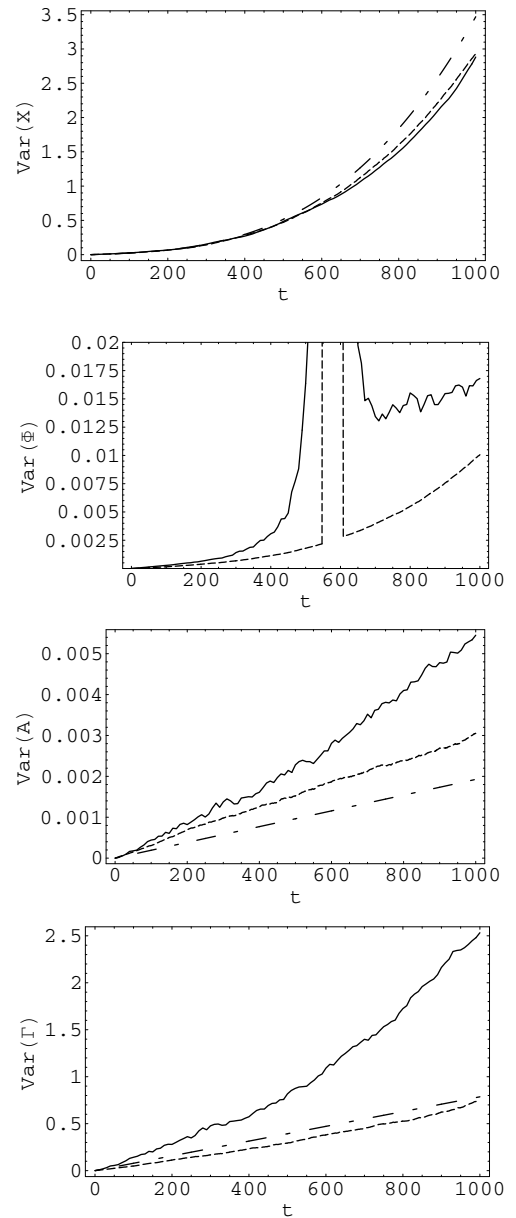


Fig. 9. Variances of the collective variables, solid line: simulations, dashed line: numerical integration of SEM 2 (38), dash-dotted line: analytical solution of SEM 1 (21), $\beta = 0.001$, $k_B T = 0.001$, $\varepsilon = 0.01$. Initial values used were $A = 1$, $\Gamma = 20$, $\Phi_0 = 0.298$.

contribute to the systematic deviations in the simulation results. As Φ_0 is calculated directly out of X , A , and Γ the fluctuations in A and Γ influence $Var(\Phi_0)$. As a consequence $Var(\Phi_0)$ is larger in the simulations than in the collective variable equations.

The peak in the variance of Φ_0 is an artifact of the measuring procedure. We apply the FORTRAN's ATAN2 function which causes jumps in Φ_0 due to its limited range $(-\pi, \pi)$. To compare the results of Φ_0 with the simulations we shuffled Φ_0 into the $(-\pi, \pi)$ range in the numerical solution of SEM 2. Therefore we observe jumps for the dashed

line in $Var(\Phi_0)$ in Figures 7 and 9 whereas in the simulations the jumps are broader. The reason for this difference is that Φ_0 does not jump simultaneously in all realizations. For some realizations the value of Φ_0 was already shifted back to the opposite end of the range, whereas this back shifting has not yet occurred for other realizations.

6 Conclusion

On a classical, anisotropic, ferromagnetic HSC with Gilbert damping and Gaussian white noise coupled magnetically to the spins, solitary waves show diffusive motion. This phenomenon was investigated analytically (for short time periods) and numerically (for longer times).

The stochastic equations of motion without damping (21) and with damping (38) are both first-order in time including intrinsic and stochastic forces. Intrinsic forces reflect interactions amongst the spins whereas stochastic forces are due to a magnetic coupling between noise terms and spins. The additional appearance of stochastic forces in A and Γ caused an indirect effect on $X(t)$ in addition to the direct effect of noise on $X(t)$. This indirect effect results in a super-diffusive contribution ($\propto t^3$) to $Var(X)$. Applying perturbative theory we solved SEM 1 analytically.

In the section applying to a longer time period we considered Gilbert damping in the LLE (11), derived the SEM 2 and solved them numerically. After comparing them to the theory we noticed a deviation in the mean values and variances of (mainly) Γ , A and Φ . This deviation is due to the sensitivity of A and Γ with respect to small fluctuations in the structure (at a given anisotropy $\beta \neq 0$) especially in the minimum of the simulated S^z configuration which is calculated by a $\text{sech}^2(x)$ fit. Inaccuracies in the calculation of the minimum lead to additional fluctuations in A and Γ so that the variances of Φ , A and Γ are always larger in the simulations than in theory. This effect is only due to the measurement of A and Γ and is therefore artificial.

However, in the mean values of all collective variables we found a good agreement between simulations and numerics. For long time periods we saw that SEM 2 describes the dynamics much better than SEM 1 since damping is considered. In fact, for the position X , which is considered the most important of the four collective variables since it is the easiest to be measured experimentally, as well as for $Var(X)$ we obtained a very satisfying agreement between spin dynamics and theory.

If we compare the anisotropic case with the isotropic one we find that the structure of the equations is very similar (due to the universality of the LLE). Thus the strategies are also very similar. The results for the dynamics of X , Φ , A and Γ are qualitatively the same. Quantitatively there are differences due to the dependence of

the diffusion coefficients on the anisotropy. This dependence has been shown explicitly; it leads to an increase of the variances of the collective variables with increasing anisotropy.

We noticed that a single-ion (on-site) anisotropy leads to several changes of the soliton properties. The soliton becomes narrower and the absolute amplitude increases. Moreover the soliton shape is stabilized against thermal fluctuations. The physical explanation is that on-site anisotropy increases the interaction of the z -components of the spins. Therefore one needs more energy to move the spin out of its z -direction.

Small fluctuations in structure lead to large fluctuations in A and Γ and consequently in Φ . Therefore the variances increase with increasing β as was observed from theory and spin dynamics simulations.

CS wants to thank Angel Sánchez (Universidad Carlos III de Madrid) for various discussions. The authors thank Chris Tarn (Universität Bayreuth) for the critical reading of this manuscript.

References

1. R. Camassa, J.M. Hyman, B.P. Luce, *Physica D* **123**, 1 (1998)
2. A.R. Bishop, J.A. Krumhansl, S.E. Trullinger, *Physica D* **1**, 1 (1980)
3. F.G. Mertens, A.R. Bishop, *Dynamics of Vortices in Two-Dimensional Magnets*, in *Nonlinear Science at the Dawn of the 21st Century*, Vol. 542, edited by P.L. Christiansen, M.P. Soerensen, A.C. Scott (Springer, 2000), p. 137
4. A.M. Kosevich, B.A. Ivanov, A.S. Kovalev, *Phys. Rep.* **194**, 117 (1990)
5. Y. Wada, *Prog. Theor. Phys. Supp.* **113**, 1 (1993)
6. N.R. Quintero, A. Sánchez, F.G. Mertens, *Phys. Rev. E* **60**, 222 (1999)
7. N.R. Quintero, A. Sánchez, F.G. Mertens, *Eur. Phys. J. B* **16**, 361 (2000)
8. M. Meister *Dissertation Zur Diffusion von Solitonen in der Heisenbergkette*, University Bayreuth, 2001
9. M. Meister, F.G. Mertens, A. Sánchez, *Eur. Phys. J. B* **20**, 405 (2001)
10. R. Rajaraman, *Solitons and Instatons* (North Holland, Amsterdam, 1998)
11. A. Sanchez, A.R. Bishop, *SIAM Rev.* **40**, 579 (1998)
12. F.G. Mertens, H.J. Schnitzer, A.R. Bishop, *Phys. Rev. B* **56**, 2510 (1997)
13. C.W. Gardiner, *Handbook of Stochastic Methods for Physics, Chemistry and the Natural Sciences* (Springer, Berlin, 1983)
14. M. San Miguel, R. Toral, in *Non equilibrium Structures VI*, edited by E. Tirapegui (Kluwer, Dordrecht, 1998)